

Retraction

Retracted: Application and Equipment of Preparation Technology of Ferroelectric Thin Film Materials in Sports Industry

Journal of Nanomaterials

Received 18 July 2023; Accepted 18 July 2023; Published 19 July 2023

Copyright © 2023 Journal of Nanomaterials. This is an open access article distributed under the Creative Commons Attribution License, which permits unrestricted use, distribution, and reproduction in any medium, provided the original work is properly cited.

This article has been retracted by Hindawi following an investigation undertaken by the publisher [1]. This investigation has uncovered evidence of one or more of the following indicators of systematic manipulation of the publication process:

- (1) Discrepancies in scope
- (2) Discrepancies in the description of the research reported
- (3) Discrepancies between the availability of data and the research described
- (4) Inappropriate citations
- (5) Incoherent, meaningless and/or irrelevant content included in the article
- (6) Peer-review manipulation

The presence of these indicators undermines our confidence in the integrity of the article's content and we cannot, therefore, vouch for its reliability. Please note that this notice is intended solely to alert readers that the content of this article is unreliable. We have not investigated whether authors were aware of or involved in the systematic manipulation of the publication process.

Wiley and Hindawi regrets that the usual quality checks did not identify these issues before publication and have since put additional measures in place to safeguard research integrity.

We wish to credit our own Research Integrity and Research Publishing teams and anonymous and named external researchers and research integrity experts for contributing to this investigation.

The corresponding author, as the representative of all authors, has been given the opportunity to register their

agreement or disagreement to this retraction. We have kept a record of any response received.

References

- [1] Y. Xu, "Application and Equipment of Preparation Technology of Ferroelectric Thin Film Materials in Sports Industry," *Journal of Nanomaterials*, vol. 2022, Article ID 9480475, 13 pages, 2022.

Research Article

Application and Equipment of Preparation Technology of Ferroelectric Thin Film Materials in Sports Industry

Yali Xu 

School of Physical Education, Jiangxi University of Chinese Medicine, Nanchang, 330004 Jiangxi, China

Correspondence should be addressed to Yali Xu; 18409484@masu.edu.cn

Received 8 March 2022; Revised 21 June 2022; Accepted 4 July 2022; Published 24 August 2022

Academic Editor: Awais Ahmed

Copyright © 2022 Yali Xu. This is an open access article distributed under the Creative Commons Attribution License, which permits unrestricted use, distribution, and reproduction in any medium, provided the original work is properly cited.

With the rapid development of the integrated circuit industry, ferroelectric thin film materials and technologies have become increasingly important. Ferroelectric materials have been widely used in aerospace, information storage, artificial intelligence, microelectromechanical, wearable devices, and other fields. Traditional sports is an important carrier of traditional culture. It contains the sports cultural resources created and precipitated by the Chinese nation for thousands of years, and all sectors of society are also paying great attention to this. Under the background of the market economy system and the major premise of the vigorous development of the cultural industry and sports industry, industrialization is obviously the inevitable choice for traditional sports to break through the difficulties and seek development, and it will also promote the further inheritance and promotion of traditional sports. The complex combination causes its performance to decrease or even fail. Therefore, it cannot cause foresee losses and disasters. It has important application value and significance to master the performance changes and mechanisms of ferrous film materials under different adding environments. This paper takes ferroelectric Pb ($Zr_{0.52}Ti_{0.48}O_3$ (PZT)Bi_{3.15}Nd_{0.85}Ti₅O₁₂(BNT) as the research object, proposes the preparation of sol coating for thin film materials, and studies the preparation parameters PZT of the sol electric ferroelectric method. Electrical method and BNT electrical film properties affect iron and physical experiments on the properties of iron. The influence of the best sol-iron coating method on the electrical properties of PZT and BNT films is the ferroelectric properties of the 700°C layer of high-temperature gas, 10-layer PZT films, and 8-layer BNT films. The elasticity and elastic moduli of PZT and BNT films are 66.8 MPa and 99.6 MPa and 159.3 GPa and 189GPa, respectively; the elastic coefficients of PZT and BNT films are 15.4×10^{10} N/m² and 18.4×10^{10} N/m², and their elastic coefficients|e31|decrease with accompanying increase in swallowing. And with the disease of reading and writing field strength, as the speed becomes faster and slower, the carriers have more time to move to the brain wall, so the intensity is also intuitive. It has strong practicability and feasibility to popularize the material and manufacture the equipment of the current sports equipment club.

1. Introduction

Intel and IBM jointly launched a 45-nanometer processor chip in 2007, using high-dielectric constant hafnium dioxide to replace the previous silicon dioxide gate insulating layer, which solves the leakage that occurs as the processor becomes smaller. This technological invention has brought historical changes to the IT industry, and the research on hafnium dioxide has also kicked off an upsurge. With the progress of people's research work, hafnium dioxide has been widely used in the fields of electronics, optics, and so

on. In 2006, Setter mentioned in a review of ferroelectric thin film materials, characteristics, and applications that ferroelectric field effect transistors (FeFET) will be used as a fast, low-energy, and nonvolatile storage technology for a long time in the future. In these devices, information will be permanently stored in the gate insulating layer in the form of polarization state and can be read nondestructively in the form of a threshold voltage change. Although as early as 1974, Wu had put forward the concept of ferroelectric field effect transistor experimentally, but for a long time, there are still many difficulties in practical application. For

example, it is difficult to obtain materials with strong stability. This is mainly due to the thermodynamic mismatch of known ferroelectric materials such as lead zirconate titanate (PZT), strontium bismuth tantalate (SBT), and strontium titanate (STO) on silicon. In addition, because silicon has a very small band step, in order to obtain low leakage current devices, thick film and precious metal electrodes must be used. In order to improve the stability of direct contact between ferroelectric materials and silicon, many methods such as the introduction of buffer layers have been tried, but these methods have reduced the scalability of such devices. To make matters worse, when the buffer layer is introduced, the existence of a higher depolarization field will degrade the information storage capacity. Therefore, in order to obtain a highly reliable ferroelectric field effect transistor, a new ferroelectric material with semiconductor compatibility is urgently needed. The ferroelectric thin film material proposed in this paper can satisfy this point. Although, in recent years, the traditional sports industry has gradually attracted the attention of people from all walks of life and has achieved certain results, but compared with the industrialization of most modern sports events, there is still a big gap. Especially in the context of the new era, how traditional sports can seize the economic and cultural double stilts to move forward steadily and realize the real industrialization of traditional sports requires further theoretical and practical discussions.

Through the investigation of the high dielectric constant gate insulating layer material, it can be found that only a few metal oxides have both semiconductor compatibility and sufficient energy band gap, and hafnium dioxide is one of them. Hafnium dioxide is an inorganic substance and an oxide of hafnium element. It is a white solid at room temperature and pressure, insoluble in water, insoluble in hydrochloric acid and nitric acid, and soluble in concentrated sulfuric acid and hydrofluoric acid. However, for a long period of time in the past, it is generally believed that hafnium dioxide does not have a noncentrosymmetric crystal structure, so hafnium dioxide cannot be a good ferroelectric material. However, many experiments in recent years have shown that hafnium dioxide-based ferroelectric thin film materials with ferroelectric properties can be obtained by controlling the material structure by methods such as doping and stress clamping. This is of great significance for the development of the next generation of ferroelectric memory that is compatible with semiconductor processes, can be miniaturized, and has low power consumption. In addition, the anti-irradiation ability of ferroelectric materials in extreme working environments has made them always regarded as one of the choices of aerospace-grade chip materials. However, after reaching a certain radiation dose, the performance of memory based on traditional ferroelectric materials will drop sharply. Therefore, research on the anti-irradiation ability of ferroelectric hafnium dioxide devices has also become very important. This research has laid the foundation for us to explore the connotation and essence of industrialization. In terms of industrialization paths, cultural industrialization paths and sports industrialization paths have always been the focus and hotspot of research, provid-

ing reference for the research on traditional sports industrialization paths.

For structures with conductive oxide (IrO_2) and metal (Pt) top electrodes, Brewer et al. studied the influence of gamma radiation on the dielectric and piezoelectric response of $\text{Pb}[\text{Zr}_{0.52}\text{Ti}_{0.48}]\text{O}_3$ (PZT) thin film stacks. When exposed to 2.5 Mrad (Si)60Co gamma radiation, the sample usually shows degradation of various key dielectric, ferroelectric, and electromechanical responses. However, the low-field, relative permittivity ϵ_r is largely unaffected by the irradiation of samples with two types of electrodes. The sample with the Pt top electrode showed a significant degradation of the remanent polarization and the overall piezoelectric response, as well as the shrinkage of the polarization hysteresis curve and the generation of multiple peaks in the dielectric constant-electric field curve after radiation. However, samples with oxide electrodes are largely unaffected by the same radiation dose, and any change in functional characteristics is less than 5%. The results show the radiation-induced changes in the number of defects or defect energy in the PZT with a metal top electrode. However, they did not consider the change and particularity of the dielectric constant of the PZT film after radiation, and there are still errors in the experiment [1]. Ferroelectric perovskite oxides are a promising photosensitive layer for photovoltaic applications due to their very high stability and the solar energy conversion mechanism associated with ferroelectrics they replace, which may lead to very high efficiency. One of the biggest challenges so far is to reduce their band gap to the visible light region while maintaining ferroelectricity. In order to solve these two problems, Pamela et al. replaced Fe with Co cations to carry out the elemental composition engineering of BiFeO_3 as a means to adjust the characteristics of transition metal-oxygen bonds. They formed an epitaxial, pure phase, and stable $\text{BiFe}_{1-x}\text{Co}_x\text{O}_3$ film through solution treatment, $x \leq 0.3$, and the film thickness is as high as 100 nm. Importantly, the band gap can be adjusted from 2.7 eV to 2.3 eV after cobalt substitution while enhancing ferroelectricity. As a proof of concept, unoptimized vertical devices have been fabricated, and it is gratifying that the electro-optic response in the visible light region of the Co-substituted. However, his method of substituting Co cations for Fe to reduce the band gap is not of high value for enhancing ferroelectricity, and further research is needed [2]. Shin and Son deposited epitaxial $\text{Bi}_2\text{FeMnO}_6$ (BFMO) film on Nb-doped SrTiO_3 (Nb:STO) substrate by pulsed laser deposition. X-ray diffraction confirmed that the 100 nm thick BFMO film has relatively high tetragonality, with a high c/a ratio of 1.04. The BFMO film has low leakage current, good ferroelectric properties and an enhanced remanent polarization of about $25.0 \mu\text{C}/\text{cm}^2$. Compared with conventional ferroelectric films (such as PbTiO_3 films), BFMO films have a larger ferroelectric domain structure due to their high domain wall energy. However, they did not make a detailed study on the ferroelectric fatigue of Nb-doped BFMO film, and there are still insufficient studies on the ferroelectric properties of BFMO film [3].

The innovation of this paper is to improve the preparation method of traditional ferroelectric thin film materials.

The sol-gel method is used to prepare ferroelectric thin films. It has precise composition control, easy adjustment, low annealing temperature, and easy to produce large-area thin films. It also has good ferroelectric properties for the prepared ferroelectric thin film. In addition, the research of this paper can also put forward suggestions for improving the equipment manufacturing and equipment production in the sports industry and provide a novel research direction for the development of sports.

2. Preparation and Performance Analysis of Ferroelectric Thin Film Materials

2.1. Ferroelectric Materials. Materials, information, and energy are the three pillars of human civilization, and materials are the material basis for the improvement of human production and living standards. The research, development, and application of new materials are the cornerstone of promoting social and technological progress. Since Schmid defined multiferroic materials in 1994 [4, 5] (referring to a class of materials with more than one ferroelectric sequence parameter for single-phase materials), the definition of multiferroic materials has been continuously broadened. At present, it is considered that the four basic order parameters of multiferroic materials are electric dipole moment, magnetic moment, elastic moment, and spin pole moment [6] (see Figure 1). That is to say, a multiferroic material is a material that has two or more basic ferroelectric characteristics (including ferroelectricity, antiferroelectricity, ferromagnetism, antiferromagnetism, and ferroelasticity). Multiferroic materials have unique physical and magneto-electric application functions, such as polarization reorientation or induction of ferroelectric phase transition under the action of a magnetic field and magnetization reorientation or induction of ferromagnetic phase transition under the action of an electric field. So they have emerged in many cutting-edge technology applications, such as sensors, energy converters, signal generation and processors, filters, information storage, and microwave devices. The research of multiferroic materials continues to attract the attention of many scholars and has become one of the key subjects of condensed matter physics and material science research [7, 8].

Multiferroic materials are mainly divided into two types: one is a single-phase multiferroic material, and the other is a composite multiferroic material. Single-phase multi-iron materials are represented by BiFeO_3 and TbMnO_3 . BiFeO_3 has ferroelectricity and antiferromagnetism at room temperature. TbMnO_3 has a large magnetoelectric coupling coefficient but a low Curie temperature. In 1972, Van Suchtelen et al. proposed a mixed preparation method of ferroelectric phase and ferromagnetic phase, which is composed of ferroelectric materials and ferromagnetic materials in different combinations. There are currently three types of structures of 0-3, 1-3, and 2-2 [9, 10], which are characterized by a relatively high Curie temperature, a large magnetoelectric coupling coefficient, and performance far higher than single-phase materials and are available for selection. Because of

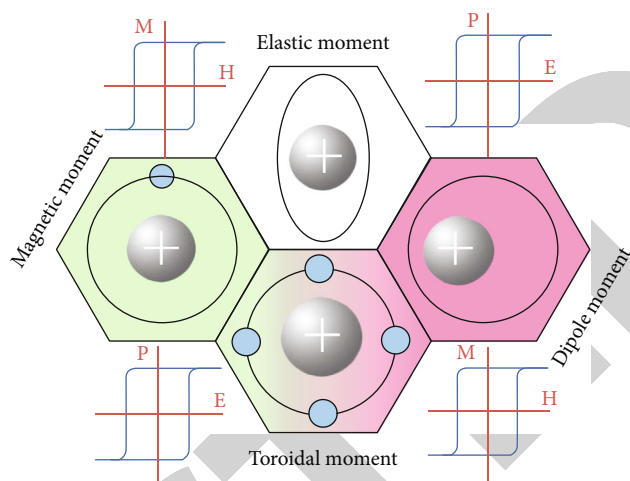


FIGURE 1: Multi-iron coupling order parameter.

this, composite multiferroic materials have become one of the hotspots in the research of multiferroic materials.

The essential feature of ferroelectric materials is the existence of spontaneous polarization, and the spontaneous polarization can change with the change of electric field [11], which is why the name of ferroelectric materials comes from. There is a hysteresis relationship between the polarization intensity of the ferroelectric material and the electric field intensity. When the polarization strength of the ferroelectric material increases, the electric field strength of the material does not increase immediately but changes only after a certain period of adaptation, as shown in Figure 2:

Ferroelectric thin films have good properties, such as ferroelectricity, piezoelectricity, pyroelectricity, electro-optics, and nonlinear optics [12, 13], and can be widely used in microelectronics, optoelectronics, integrated optics, and microelectronic mechanical systems. Other fields are currently one of the frontiers and hotspots of high-tech research [14].

After nearly a century of development, ferroelectric materials have formed five major types of structural systems: perovskite type, lithium niobate type, bismuth-containing layered, pyrochlore type, and tungsten bronze type structure system [15, 16]. Perovskite-type ferroelectrics are currently the most widely used, perfect perovskite structure, usually expressed by ABO_3 . At present, the main research is barium titanate (BaTiO_3), lead titanate (PbTiO_3), and other representative perovskite-type ferroelectric materials, as well as their performance research such as A/B and AB position ion substitution [17, 18].

2.2. Test and Characterization Methods of Thin Film Materials and Development Overview. In recent years, the application of ferroelectric thin film materials has gradually increased. In the aerospace, automotive, and sports industries, ferroelectric thin film materials have potential applications. With the maturity of the preparation process of ferroelectric thin film materials, the performance of this material has been greatly improved. Its piezoelectric effect, pyroelectric effect, electro-optic effect, and acousto-optic

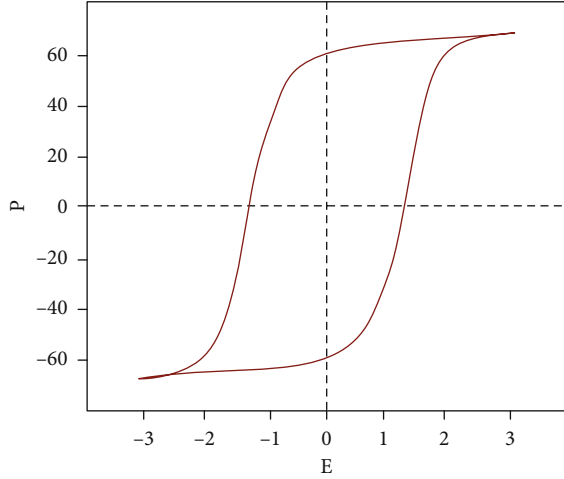


FIGURE 2: Hysteresis loop diagram of ferroelectric materials.

effect have been developed relatively maturely. And the cost has been greatly reduced, so its application fields have been expanded, and it can be used to manufacture precision parts for microwave circuit plug-ins and turbocharged propulsion. There are also reports on their applications in the sports industry and electronic fields. In the sports industry, the use of nanomaterials to develop volleyballs that do not touch water and dust is more conducive to the promotion of sports activities. Performance characterization (detection and evaluation) is particularly important for the future application of materials. It is not only related to the correct evaluation of materials but also lays the foundation for the design and application of materials. The detection and evaluation of materials has a wealth of content, such as the detection and analysis of key issues such as elastic modulus, plastic strain, fracture toughness, and fatigue [19, 20]. At present, the application scope of ferroelectric thin film and magneto-electric composite thin film involves all aspects of functional thin film materials and devices. It is represented by applications in the fields of microelectromechanical systems, sensors, detectors, and information storage. It is constantly advancing social progress and changing people [21]. Therefore, it is indispensable to understand the mechanical parameters of thin film materials such as elastic modulus, Poisson's ratio, residual stress, fatigue strength, and fracture strength before designing and manufacturing new materials and devices. The mechanical properties of thin film materials directly affect the quality of new materials and devices. The traditional testing methods are mostly suitable for bulk materials, which poses great challenges to the mechanical parameter testing of microcomponents and functional thin-film devices [22, 23].

2.3. Application of Ferroelectric Thin Film. In previous studies, significant progress has been made in the preparation of ferroelectric thin films, the synthesis of multilayer films, performance, testing, microstructure, and the integration of ferroelectric thin films into heterostructures [24]. The discovery of $\text{SrBi}_2\text{Ta}_2\text{O}_9$ (SBT) makes FRAM very suitable for its excellent fatigue resistance, excellent storage perfor-

mance, and low leakage current. However, the use of ferroelectric thin films is not limited to ferroelectric memories [25]. Utilizing the dielectric, ferroelectric, piezoelectric, electrostatic, pyroelectric, optical, electro-optical, and other properties of ferroelectric film, its application is extended to separation devices [26]. In this way, the main application of ferroelectric film in the memory of multilayer capacitors, nonvolatile ferroelectric dynamic random access memory (NVRAM), smart cards, infrared detectors, infrared sensors and inverters, etc., will be extended. According to the physical results, the application of ferroelectric thin film can be classified as shown in Table 1.

New applications of ferroelectric thin films are still being proposed, such as the use of iron thin films such as laser disks, microwave waveguides, solar cell energy storage capacitors compatible with solar cells, and powerful electron emission sources [27].

2.4. Methods of Fatigue Characteristics of Ferroelectric Capacitors. The relationship between temperature and fatigue rate, when the temperature rises, the fatigue rate also rises rapidly. It can be expressed as

$$T(A) = T_0 \times [1 - R(S) \times \log A]. \quad (1)$$

Among them, T_0 is the initial residual polarization, $T(A)$ is the residual polarization after reading and writing, and $R(S)$ is a temperature-dependent phase.

$$\varepsilon_d \mu R(S) = A \times \exp \left[-\frac{B_a}{k_b T} \right]. \quad (2)$$

Among them, B_a is the activation energy, T is the temperature in Kelvin, K_B is the Boltzmann constant, and A is a proportional coefficient.

In this study, similar electrical performance characterization was performed on the devices before and after fatigue, and the modified SE model was used to fit the measured current under low field. The following can be drawn:

$$\ln \left(\frac{R_{SE}}{T^{2/3}} \right) = \ln(D(S)) - \frac{A}{DT} \left[\left(\sqrt{\frac{AB}{4\pi\varepsilon_0^2\varepsilon_d\varepsilon_{st}}} \right) - b\sqrt{V} \right], \quad (3)$$

$$D(S) = 2a \left(\frac{2\pi m_{\text{eff}} d}{h^2} \right)^{3/2} \mu E, \quad (4)$$

$$b = \sqrt{\frac{a^2 N_{\text{eff}}}{8\pi\varepsilon_0\varepsilon_d B}}, \quad (5)$$

$$\log \left(\frac{R_{PF}}{E} \right) = \frac{[-a[\varphi_t - (aE/\pi\varepsilon_d\varepsilon_0)^{1/2}]]}{D_B T \ln 10} + \log(B), \quad (6)$$

where m_{eff} is the effective mass of electrons, D_B is Boltzmann's constant, h is Planck's constant, μ is the mobility of carriers in the film, E is the applied field strength, φ_B is the barrier height at the interface, φ_t is the bound energy

TABLE 1: Application of ferroelectric thin film.

Performance	Main components
Dielectric	Capacitors, dynamic random access memory (DRAM)
Piezoelectricity	Surface acoustic wave (SAW) devices, miniature piezoelectric motors, miniature piezoelectric actuators
Pyroelectricity	Pyroelectric detector and array
Ferroelectricity	Ferroelectric random access memory (FRAM)
Electro-optic effect	Optical modulator, optical waveguide
Acousto-optic effect	Acousto-optic deflector
Photorefractive effect	Optical modulator, optical holographic memory
Nonlinear optical effect	Optical frequency doubler

level in the material, ϵ_0 is the dielectric constant in vacuum, ϵ_d is the dynamic dielectric constant of the ferroelectric material in the infrared region, ϵ_{st} is the static dielectric constant of the ferroelectric material, and N_{eff} is the depletion layer at the cross section charge density, including bound charge and shallow ions. B is the remanent polarization of the ferroelectric material, S is the applied voltage, and A is the unit point charge. The improved SE model takes into account the influence of polarization at the metal-ferroelectric-metal interface on the maximum field strength. If the ferroelectric polarization is not taken into account, the calculated Schottky barrier will be much lower than the actual one.

The next step will be to discuss the situation in the low field. According to the improved SE model, the magnitude of the tunneling current mainly depends on the free carriers of the injected metal passing through the Schottky barrier of the ferroelectric layer interface. The larger the actual value of the Schottky barrier, the smaller the value of the tunneling current. Here, first define the "significant" barrier ϕ :

$$\sigma_{ie} = \sigma_b - \sqrt{\frac{aB}{4\pi\epsilon_0^2\epsilon_d\epsilon_{st}}}. \quad (7)$$

The value at each voltage can be obtained by fitting the slope of the straight line.

The Seebeck effect, as the most basic theoretical basis for ferroelectric performance, was first discovered by Seebeck in 1821. When two different materials are connected end to end into a closed loop, two connection points are formed. The two connection points are made by certain means. If the temperature difference is formed at the position, then an electric current is formed in the closed circuit. It can be expressed by a formula:

$$G_{iu} = \alpha_{ab}(C_1 - C_2), \quad (8)$$

where α_{ab} is the thermoelectromotive force rate. For the same material, when it approaches zero, α_{ab} can be regarded as a constant, which is named Seebeck coefficient, namely,

$$\alpha_{ab} = \lim_{\nabla C} \frac{G_{iu}}{\nabla C} = \frac{dv_{iu}}{dc}. \quad (9)$$

In a certain period of time, the change in heat at the connection point in the entire closed loop, that is, the transfer of heat is proportional to the current, and the ratio of the change in heat at the connection point Rt to the current I in unit time R_d is

$$\frac{R_d}{Rt} = \pi I, \quad (10)$$

where π is the Peltier coefficient, the unit is V, and its magnitude is related to the material and voltage of the closed loop.

The Thomson effect, which is a secondary thermal effect, when a current flows through a uniform conductor with a temperature gradient, in addition to generating Joule heat related to resistance, the conductor also absorbs or releases heat. This effect of absorbing or releasing heat is called the Thomson effect. It has a small heat absorption and release and is reversible, so it is very difficult to measure and easily confused with Joule heating.

$$\frac{R_d}{Rt} = \tau I \left(\frac{R_t}{t} \right). \quad (11)$$

The three do not exist independently of each other but are inseparable from the mutual influence of the three of the same substance. The relationship between them is

$$\pi_{ab} = \alpha_{ab} C, \quad (12)$$

$$\frac{d\alpha_{ab}}{dC} = \frac{\gamma_a - \gamma_b}{C}. \quad (13)$$

It can be seen that the three-point iron effect is reversible, and the Joule heat generated by the internal resistance of the material corresponding to it is irreversible.

The thermoelectric conversion device can directly convert heat energy and electric energy, and it provides a scalable, reliable, and environment-friendly energy conversion method. The conversion efficiency of the thermoelectric conversion device can be determined:

$$\lambda = \frac{P_e - P_o}{P_e} \times \frac{\sqrt{1 + ZP} - 1}{\sqrt{1 + ZP} + (P_e/P_o)}, \quad (14)$$

where P_e and P_o are the temperature of the hot and cold ends of the ferroelectric material and the ZP value is a dimensionless thermoelectric figure of merit. It is the decisive factor that determines whether the thermoelectric material can be widely used. Its size can be defined as

$$ZP = \frac{\delta^2}{d}, \quad (15)$$

where P is the average temperature, which reflects the electrical transport characteristics of the thermoelectric material, and d is the thermal conductivity, which reflects the heat transport characteristics of the material.

2.5. Ferroelectric Thin Film Materials in Sports. At present, ferroelectric thin film materials are widely used in sports measurement sensors. It has both piezoelectricity and mechanical properties of soft film. Pressure sensors made with it can be used to detect human body signals such as pulse and heart sounds. The pulse and heart sound signal carries important physiological parameter information of the human body. Through effective processing of the signal, the waveform and the number of heart rate can be accurately obtained, which can provide a reliable basis for physical fitness measurement. In addition, sensors made of ferroelectric thin-film materials have a large frequency response range, pyroelectric effect, and other characteristics and have great application potential. In terms of vibration detection, it is mainly used in music pickup, machine condition monitoring, bearing wear, fan airflow, rope breakage, etc., as an accelerometer in acceleration detection and in nondestructive testing. When it appears in the form of a sensor array, it can also be used to monitor human movement, sports scoring, switches, and microphones. With the improvement of the production process of ferroelectric thin film materials, the continuous decline of production costs, and the continuous development and in-depth research in various aspects, it is reasonable to believe that the application prospects of ferroelectric thin film materials in the sports industry must be very broad.

3. Preparation of Ferroelectric Thin Film

3.1. Film Preparation Method. Although the pulsed laser deposition (PLD) film-making technology has only a history of more than 50 years, it is a promising manufacturing technology with distinct advantages and disadvantages. The main advantages are as follows: (1) the element measurement ratio of the film material and the target material can be consistent under appropriate conditions. (2) It can prepare many inorganic thin film materials such as refractory materials, metals, semiconductors, insulators, and some organic thin film materials. (3) Multilayer films, heterogeneous films, etc., can be prepared, and the target change is convenient and flexible. (4) It is convenient to adjust the deposition parameters and growth rate, the deposition temperature is low, and the film quality is high. The disadvantages are also obvious: the uniformity of the film formation

is poor, the formation of a large area film is difficult, and mass production and preparation cannot be carried out.

The sputtering method started in 1940 and developed rapidly with the rise of the semiconductor industry and was officially born in the 1970s. Its advantages are mainly reflected in the following: (1) the film-forming temperature is usually lower than 500°C; it is compatible with microelectronics technology and can be used to make devices. (2) The prepared film is of good quality without pinholes and cracks. (3) The crystallization performance is good, and an epitaxial single crystal film can be obtained. The main disadvantages are slow film growth rate, long preparation time, deviation of film composition and target material, etc.

Metal organic chemical meteorological deposition (MOCVD) uses metal organic compounds as the material source for chemical vapor deposition. After more than 30 years of development, it has been relatively perfect. The method can precisely control the composition and thickness of the thin film; it is easy to produce a large-area film, the deposition temperature is low, and the uniformity and repeatability of the prepared thin film are high. However, due to the high toxicity of raw materials and the high cost of materials and equipment, the application scope of MOCVD is limited.

The sol-gel method uses inorganic metal salts or metal alkoxides prepared with liquid chemical reagents as solvents and alcohol solutions as solvents, and the two are mixed. After a series of hydrolysis, carbonization, and carbonization reactions, they are transparent and uniform. Use different methods. The precursor solution is aged; then, the precursor solution matures to polymerize and gel the solute; finally, the gel is dried and baked to remove organic compounds and obtain a thin film material. The processing equipment requirements are simple and easy to apply. The chemical uniformity is good and can reach the molecular level. The stoichiometry is accurate, quantitative and uniform doping can be achieved, the doping range is wide, the manufacturing temperature is low, and it is compatible with semiconductors. The sol-gel method also has certain limitations. The alkoxides that can be selected are limited, expensive, and easy to pollute the environment; during the drying process, organic matter volatilizes and cracks occur; when different materials are prepared, it is difficult to control the changes in process parameters. The above four methods for preparing ferroelectric thin films have their own advantages and disadvantages, and they need to be selected according to different needs. The bulging sample is a self-clamping free film, which is prepared by chemical etching in the later stage. At the same time, it is necessary to quickly prepare a film sample with good uniformity and stable performance. These differences indicate that the preparation method also has a certain impact on the performance of the material.

In Table 2, various properties under different preparation processes are compared. It can be seen that the film prepared by the sol-gel method has higher remanent polarization, and it also has the smallest coercive field and the largest dielectric constant. It reached 0.8 and 46, respectively. These indicators are important because a higher

TABLE 2: Comparison of film properties under different preparation methods.

	PLD	Sputtering	MOCVD	Sol-gel
2Pr (C/cm ²)	49	23	27	29
Rectify the field (MV/cm)	1.2	0.9	2.1	0.8
Dielectric constant	44	31	24	46

residual polarization means a larger read and write window, a smaller coercive field means lower power consumption, and a higher dielectric constant means smaller leakage. Therefore, this paper chooses the sol-gel method as the method of preparing the film.

3.2. Preparation of Sol-Gel Film

3.2.1. *Experimental Supplies.* The chemicals used in the experiment are shown in Table 3.

During the reaction process, a certain chelating agent (acetylacetone) is added to the solution to control the polycondensation rate and hydrolysis rate of the alkoxide while also keeping the titanium and zirconium ions in a stable state to obtain a uniform gel. After adding a certain amount of acetic acid, it can not only adjust the pH of the solution but also act as a catalyst.

Pt metal has stable properties and low diffusion performance and can prevent mutual diffusion between interfaces. The atomic weight of platinum is 195.078, which is slightly smaller than that of gold, and the atomic number is 78, which belongs to the transition metal. Therefore, Pt thin film is selected as the bottom electrode of the substrate. At the same time, the Ti film is selected as the buffer layer connecting SiO₂/Si to enhance the bonding strength of the Pt layer. The substrate used in the experiment was provided by Peking University Microelectronics, and the structure from top to bottom was Pt/Ti/SiO₂/Si/SiO₂, as shown in Figure 3. The total thickness is 500 μm, the thickness of the Pt layer is 150 nm, the thickness of the Ti layer is 20 nm, the thickness of the SiO₂ layer is 20 μm, and the preferred orientation of the Pt layer is (111).

3.2.2. *PZT Film Preparation.* For the preparation of PZT film precursor, the selected composition ratio is Pb:Zr:Ti=1.15:0.52:0.48, which is near the quasihomotype phase boundary. An excess of 15% of lead is used to suppress the formation of oxygen vacancies caused by lead volatilization during annealing. The preparation steps of the PZT precursor solution are as follows:

- (1) Use an electronic balance to weigh out 3.774 g lead acetate, 2.009 g zirconium nitrate, and 1.500 g butyl titanate. Dissolve zirconium nitrate and butyl titanate in ethylene glycol methyl ether solution and stir evenly. Add 3 to 5 drops of acetylacetone to the butyl titanate solution as a stabilizer
- (2) Lead acetate is relatively insoluble, so after it is dissolved in ethylene glycol methyl ether, it is heated in a hot water bath while stirring on a magnetic stir-

rer. The temperature is set to 60°C, and it is completely dissolved and placed at 120°C. Dry in a vacuum drying oven (model DZF-6020) for 5~10 min to remove crystal water, and then add a little glacial acetic acid after cooling to room temperature

- (3) Slowly dissolve the zirconium nitrate solution in the lead acetate solution, stir it evenly, and then add the butyl titanate solution to the mixed solution to form a light yellow precursor solution
- (4) Add a proper amount of ethylene glycol methyl ether to adjust the concentration of the precursor solution to 0.3 mol/L, and add a proper amount of formamide to prevent the prepared film from cracking. After continuous stirring for 8-10 h, aging for 4-7 days, the solution is a light yellow transparent liquid without precipitation, and the preparation is complete. The flow chart is shown in Figure 3

3.2.3. *Preparation of BNT Film.* The preparation of BNT film precursors is relatively simple, and the preparation steps are as follows:

- (1) According to the stoichiometric ratio of Bi_{3.15}Nd_{0.85}Ti₃O₁₂, weigh appropriate amounts of nitric acid (Bi(NO₃)₃·5H₂O) and neodymium nitrate (Nd(NO₃)₃·6H₂O), of which bismuth nitrate is weighed 10% more to make up Bi element volatilization loss during subsequent processing
- (2) Place the weighed sample in a clean beaker, add 5 mL of glacial acetic acid and 4 mL of ethylene glycol methyl ether to the beaker, respectively, and place it on a magnetic stirrer and stir (the solution is purple), which is the A solution
- (3) In another clean beaker, add 4 mL of ethylene glycol methyl ether and 4 drops of acetylacetone, stir appropriately to make the mixture even. After peeling the skin on the electronic balance, add a certain weight of butyl titanate (C₁₆H₃₆O₄Ti) solution to the beaker to form solution B
- (4) After stirring the A and B solutions for 5-10 minutes, slowly add the A solution to the B solution to obtain a mixed solution (wine red), and adjust the concentration to 0.01 mol/L. Stir on a magnetic stirrer for 5 to 8 hours, and a light yellow BNT precursor will be obtained. Let it stand for 4 to 7 days to age the solution. If no precipitation appears, the preparation is complete. The schematic diagram of the process is shown in Figure 4

After the preparation of the precursor solution is completed, the preparation of the film can be carried out. The spin-coating preparation process is carried out in an ultra-clean room, which has a grade of 10,000. The homogenizer is a KW-4B homogenizer produced by Beijing Saidecase Electronics Co., Ltd. When the film is prepared by the spin

TABLE 3: Summary of experimental drugs.

Drug name	Molecular formula	Purity	Molar mass (g/mol)
Zirconium nitrate	$Zr(NO_3)_4 \cdot 5H_2O$	Analytically pure	425.16
Lead acetate	$(CH_3COO)_2Pb \cdot 3H_2O$	99.1%	383.25
Butyl phthalate	$C_{16}H_{36}O_4Ti$	98.7%	351.67
Neodymium nitrate	$Nd(NO_3)_3 \cdot 6H_2O$	98.5%	328.16
Bismuth nitrate	$Bi(NO_3)_3 \cdot 5H_2O$	99.3%	491.38
Ethylene glycol monomethyl ether	$C_3H_8O_2$	99%	77.41
Acetylacetone	$C_5H_8O_2$	98%	101.79
Formamid	CH_3NO	Analytically pure	48.35
Acetic acid	CH_3COOH	Analytically pure	62.83

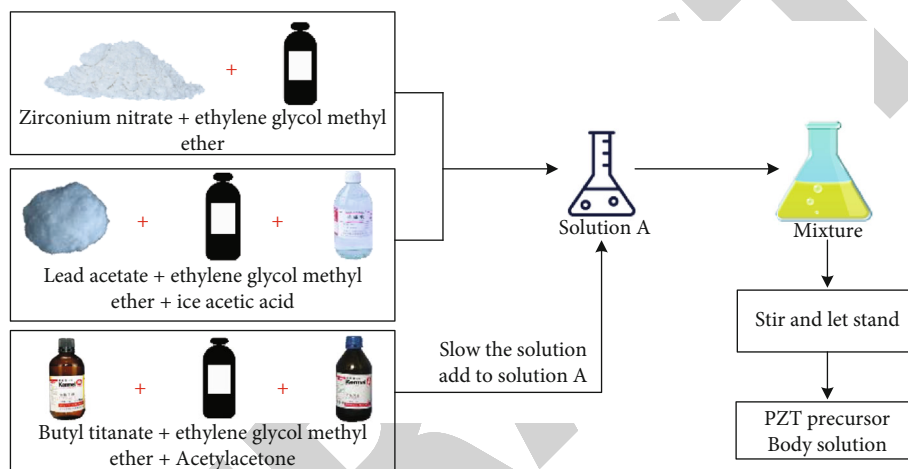


FIGURE 3: Schematic diagram of the preparation process of PZT precursor solution.

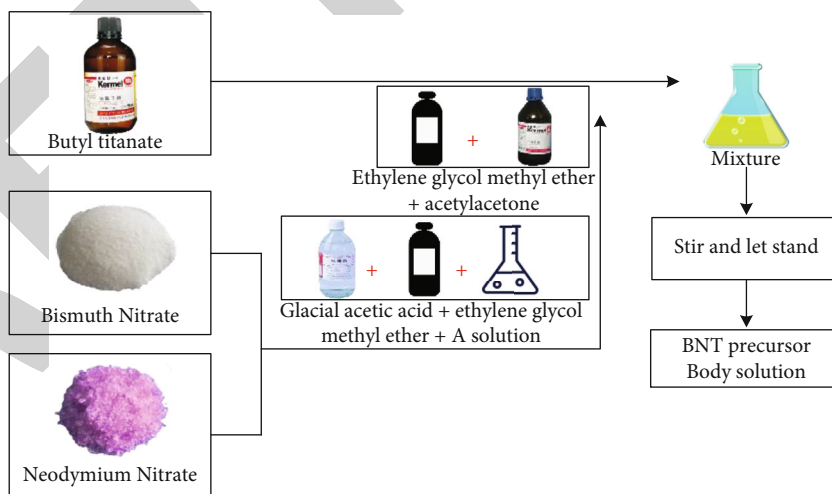


FIGURE 4: Schematic diagram of the preparation process of BNT precursor solution.

coating method, the effect of the parameter setting of the homogenizer on the performance of the film is mainly reflected in the uniformity of the film, and the annealing process mainly controls the ferroelectric properties of the film, such as the size and orientation of the crystal grains, and the defects in the film.

After many experiments and comparisons with other documents, the spin coating process parameters are set to low speed 400 r/s and high speed 4000 r/s, and the spin coating time is 10 s and 40 s, respectively. The air humidity in the ultraclean room is controlled between 39% and 48%, the temperature is changed between 17.4 and 22.2°C, and the

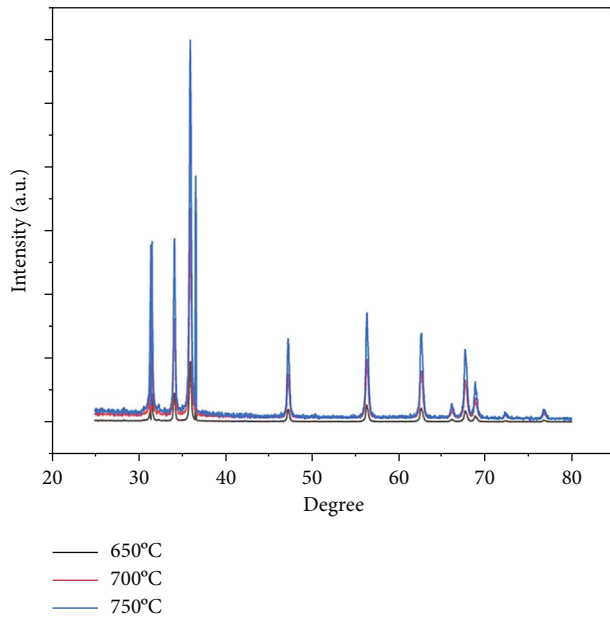


FIGURE 5: XRD pattern of PZT film under air and oxygen annealing atmosphere.

humidity and temperature remain basically unchanged during a single spin coating. The rapid annealing process is divided into three small stages: the first stage is drying, and 18 s is heated from room temperature to 180°C and maintained for 300 s; the second stage is pyrolysis, and 20 s is heated from 180°C to 400°C and maintained for 300 s; the third stage is annealing, and 20 s is heated from 400°C to 700°C and kept for 600 s; that is, a complete annealing is completed.

When the spin coating reaches the desired thickness, the annealing process is completed, and the film preparation is completed. The Ni layer in the Ni/PZT composite film is sputtered by the MIS800 multifunctional ion beam magnetron sputtering composite coating equipment. The sputtering voltage is 2 kV, the current is 50 mA, and the sputtering time is 20 min. The thickness is about 100 nm, and then, a 5–10 nm Ag layer is covered on the surface of the nickel layer as a protective layer to prevent oxidation of the nickel layer.

4. Influence of Preparation Parameters on the Ferroelectric Properties of PZT Thin Films

4.1. Effect of Annealing Environment on the Ferroelectric Properties of PZT Thin Films. When annealing at the same temperature, the environment of the sample can also affect the intrinsic properties of the film, and the difference in oxygen partial pressure will produce different effects. Figure 5 shows the XRD pattern of the PZT film under annealing environment.

Annealing in air has a low oxygen partial pressure, and there are usually more oxygen vacancies generated during annealing, resulting in more defects in the film; the existence of defects will increase the leakage current of the film, reduce the polarization of the film, and reduce the residual polariza-

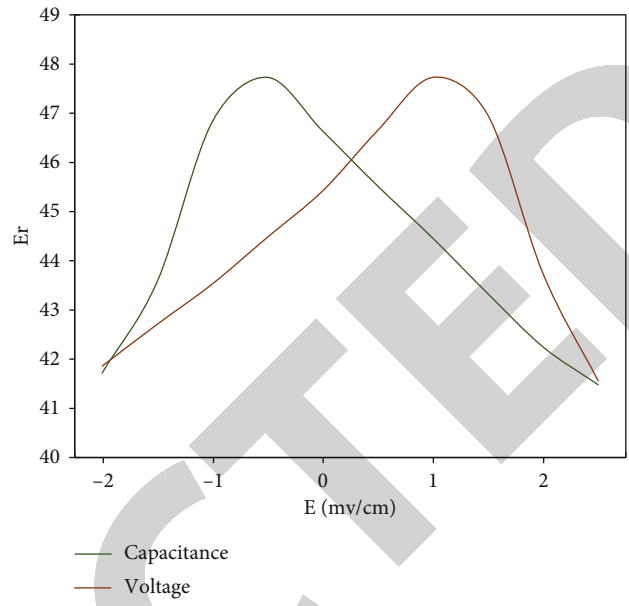


FIGURE 6: Ferroelectric thin film C-V test.

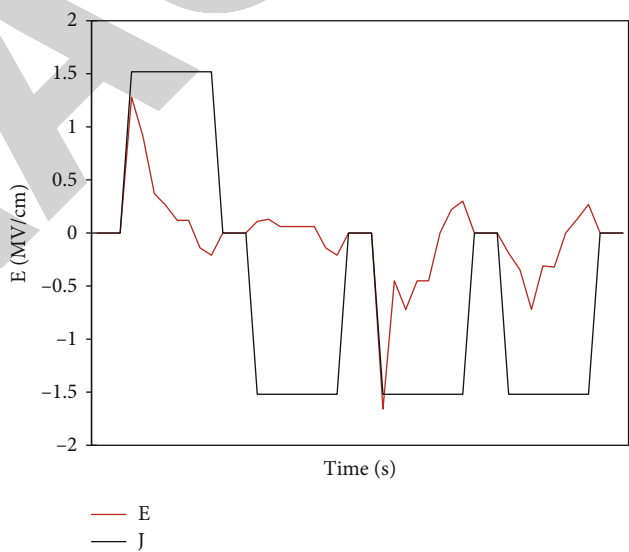


FIGURE 7: PUND test displacement current result.

tion. The value becomes smaller; at the same time, the increase of defects makes the clamping effect more significant and inhibits the reversal of the ferroelectric domain, and the electrical domain reversal is difficult; that is, the electrical coercive field of the ferroelectric film becomes larger. Annealing in an oxygen atmosphere significantly increases the oxygen partial pressure ratio, inhibits the generation of oxygen vacancies, and reduces the number of internal defects in the film, making the film denser and improving the ferroelectric properties.

4.2. Structure and Conductivity of Ferroelectric Thin Films. First, the structure and ferroelectric properties of the prepared ferroelectric thin film were characterized.

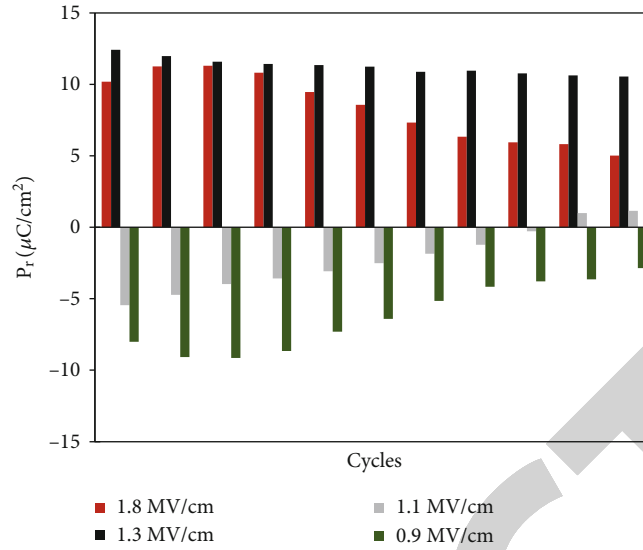


FIGURE 8: The relationship between the residual polarization intensity and the number of reads and writes under different pulse amplitudes.

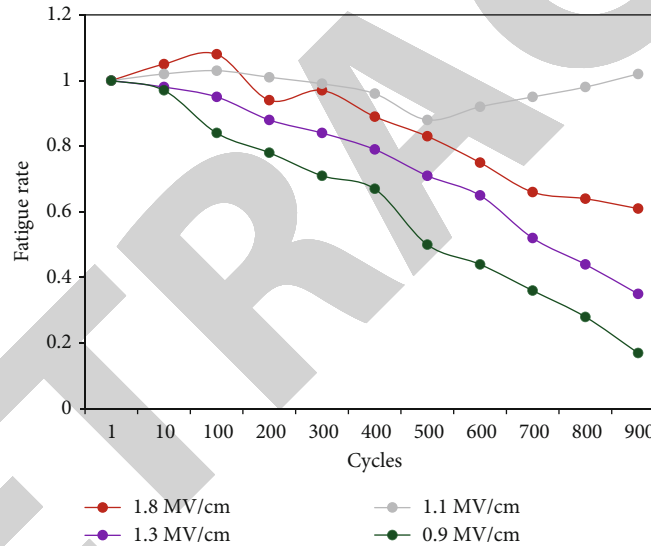


FIGURE 9: Normalized results of fatigue rate under each pulse amplitude.

Figure 6 shows the capacitance-voltage test of the prepared 15 nm thick sample. The electrode area of the test device is $30 \mu\text{m} \times 30 \mu\text{m}$, the applied field strength range is $\pm 3 \text{ MV/cm}$, and the test frequency is 50 kHz. From the figure, you can see a “butterfly-shaped” CV curve unique to ferroelectric materials. Two obvious “bulges” can be observed around $\pm 0.8 \text{ MV/cm}$, which is a characteristic of ferroelectric capacitors. The reason is that the movement of the domain wall near the coercive field will increase significantly.

Figure 7 shows the displacement current during the PUND (positive up, negative down) test. A polarization current of about 0.1 A cm^{-2} can be observed at the rising edge of the first positive pulse and the falling edge of the third pulse, which is also one of the current characteristics of ferroelectric materials.

4.3. Fatigue Characteristics Analysis of Ferroelectric Capacitors. In PZT-based ferroelectric capacitors, there have been many reports that the rate of device fatigue is closely related to pulse width, pulse amplitude, and temperature. These characteristics are related to various fatigue mechanisms such as domain wall pinning, redistribution, and injection of oxygen vacancies.

In this experiment, the fatigue characteristics of the device were also characterized under these different experimental conditions. The first research is the relationship between fatigue characteristics and pulse amplitude. The frequency of the pulse is fixed at 0.91 MHz, as shown in the inset in Figure 8; the amplitude of the pulse varies from $0.8 \text{ MV}\cdot\text{cm}^{-1}$ to $1.8 \text{ MV}\cdot\text{cm}^{-1}$, as shown in Figure 8. In the literature, hafnium dioxide-based ferroelectric materials will have the characteristic of “wake-up” in the polarization

TABLE 4: Comparison of device performance indicators under different irradiation doses.

Dose(ions/cm ²)	Dielectric constant	Coercive field (MV/cm)	2Pr ($\mu\text{C}/\text{cm}^2$) (at 2.5 MV/cm)	2Pr ($\mu\text{C}/\text{cm}^2$) (at 1.3 MV/cm)	2Pr after cycling ($\mu\text{C}/\text{cm}^2$) (at 1.3 MV/cm)		
					Mean values	Range	Percentage
Initial state	39.4	1.12/-0.68	24.9	13.9	1.5 ~ 5.5	2.75	23%
5×10^{13}				12.6	2.1 ~ 8.8	4.66	36%
10^{14}	39.2	1.19/-0.56	24.4	11.4	3.6 ~ 10	4.78	54%
5×10^{14}				10.7	1.6 ~ 8.4	5.52	43%
10^{15}	38.8	1.07/-0.59	23.6	9.8	1.2 ~ 6.6	3.24	26%

intensity during the first 200 reads and writes; that is, the polarization intensity will first increase with the increase in the number of reads and writes. This phenomenon has also been observed in this experiment. When the reading and writing field strength is $1.8 \text{ MV}\cdot\text{cm}^{-1}$, the residual polarization intensity increases from $12 \mu\text{C}\cdot\text{cm}^{-2}$ to $13 \mu\text{C}\cdot\text{cm}^{-2}$ after reading and writing 200. It was also at this moment that fatigue began to occur. When the reading and writing field strength is reduced to below $1.3 \text{ MV}\cdot\text{cm}^{-1}$, the “wake up” phenomenon disappears, and the device shows fatigue characteristics directly from the beginning of reading and writing. When the reading and writing field strength decreases from $1.8 \text{ MV}\cdot\text{cm}^{-1}$ to near $0.9 \text{ MV}\cdot\text{cm}^{-1}$ of the material coercive field, the fatigue rate increases significantly.

Figure 9 normalizes the fatigue rate under various field strengths ($P(N)/P_0$, where $P(N)$ represents the residual polarization after reading and writing N times and P_0 represents the initial residual polarization of the device). It can be seen very clearly that as the reading and writing field strength decreases, the fatigue rate of the device is gradually increasing.

In this paper, the fatigue characteristics are studied, and it can be seen that the device is more likely to exhibit fatigue characteristics at a voltage close to the coercive field. Therefore, in order to better study the characteristics of fatigue characteristics under proton irradiation, in this chapter, we have carried out fatigue tests on the device near the coercive field, and we can see that the fatigue has a tendency to first improve and then decrease.

Table 4 summarizes the changes of various ferroelectric properties under irradiation. It can be seen that the dielectric constant, the coercive field, and the residual polarization under $2.5 \text{ MV}\cdot\text{cm}^{-1}$ only slightly changed. Irradiation even has an inhibitory effect on fatigue. In general, the performance of devices based on ferroelectric thin films does not change significantly under proton irradiation.

5. Conclusions

Ferroelectric thin film materials can greatly improve the overall performance of sports facilities, improve sports equipment, improve the quality of new equipment, and promote athletes to obtain excellent results. Therefore, the application of ferroelectric thin film materials to sports will have a lasting high-quality impact on the sports industry. Ferroelectric thin film materials have great potential and can improve all aspects of sports. Sports activities require

specific equipment and equipment, as well as the material texture and design of the equipment, which play a vital role in the development of sports. The application of ferroelectric thin film materials in the sports industry is mainly reflected in two aspects: one is the application in sports infrastructure, such as the construction of sports venues, sports equipment, sports clothing, and sports biology. The second is the application in sports equipment, such as enhanced golf, tennis, swimming, racing, and cycling. The core part of sports industrialization refers to the industrial phenomenon that a certain sports event takes competition activities as the leader, achieves a high degree of marketization, and forms a considerable economy of scale, thus presenting an industrial phenomenon. Such industrialization has played a decisive role in the development of sports. The extension of sports industrialization refers to the industrialization of all sports-related departments. They will promote the development of sports, but they are not decisive. The industrialization of sports is the same as the socialist modernization construction in China. Its foothold can only be based on the national conditions. The industrialization of sports can only give full play to its own advantages and adapt to the requirements of the socialist market economy only if it conforms to the national conditions. Its basic feature is that the industrialization of sports is a direction for China to deepen the reform of sports. It is the process of sports from a closed system run by the state to an open system run by the state and society. What needs to be emphasized is the social and economic benefits of sports. In this paper, PZT and BNT ferroelectric films were prepared by sol-gel method, and PZT and BNT were used as the research objects to study the influence of sol-gel method preparation parameters on the properties of PZT and BNT ferroelectric films. When the annealing temperature increases, the degree of crystallization of the film increases. When the film is annealed in an oxygen atmosphere, the oxygen partial pressure increases, reduces the oxygen vacancy concentration, suppresses the occurrence of defects, and improves its ferroelectric properties. The increase of film thickness can increase the average size of crystal grains, reduce the internal stress of the film, and also improve the ferroelectric properties of the film. When annealed in an oxygen atmosphere at 700°C and a thickness of 10 layers, the ferroelectric properties of the PZT film are the best. The BNT film has the best ferroelectric performance when it is annealed in an oxygen atmosphere at 700°C , and the thickness is 8 layers. Then, using electrical characterization and other methods to study its fatigue

mechanism and anti-irradiation performance, it is concluded that the occurrence of the ferroelectric film fatigue process is closely related to the magnitude of the applied field strength, the frequency of read and write pulses, and the temperature, and these characteristics all point to the main fatigue mechanism caused by charged carrier injection. The performance of the device is stable under proton irradiation, and the fatigue characteristics are even improved. This paper studies the excellent performance characteristics of ferroelectric thin films that can be used in the optical and sensing sports industry. Sensors made of ferroelectric thin film materials have sufficient sensitivity and accuracy to perform online in-body monitoring and are widely used in the sports industry. However, there are still some shortcomings in the research of this paper. Although the mechanism of ferroelectric thin film fatigue is proposed in this paper, the improvement of fatigue has not been achieved. It is hoped that this problem that hinders commercial application can be completely solved in future work. And in future research work, I will propose methods for ferroelectric material optimization from more perspectives based on existing technologies and methods and continuously improve the quality and efficiency of research work.

Data Availability

No data were used to support this study.

Conflicts of Interest

There is no potential conflict of interest in this study.

References

- [1] S. J. Brewer, C. Z. Deng, C. P. Ca Llaway, M. K. Paul, K. J. Fisher, and R. Q. Rudy, "Effect of top electrode material on radiation-induced degradation of ferroelectric thin film structures," *Journal of Applied Physics*, vol. 120, no. 2, p. 024101, 2016.
- [2] M. Pamela, S. Mateusz, and G. Jaume, "Band gap tuning of solution-processed ferroelectric perovskite $\text{BiFe}_{1-x}\text{Co}_x\text{O}_3$ thin films," *Chemistry of materials: a publication of the American Chemical Society*, vol. 31, no. 3, pp. 947–954, 2019.
- [3] H. W. Shin and J. Y. Son, "Large ferroelectric domain structures of epitaxial $\text{Bi}_2\text{FeMnO}_6$ thin films on Nb-doped SrTiO_3 substrates," *Journal of Materials Science*, vol. 28, no. 20, pp. 15302–15305, 2017.
- [4] L. X. Chen, C. Xu, X. L. Fan, X. H. Cao, K. Ji, and C. H. Yang, "Study on leakage current, ferroelectric and dielectric properties of BFMFO thin films with different bismuth contents," *Journal of Materials Science: Materials in Electronics*, vol. 30, no. 8, pp. 7704–7710, 2019.
- [5] V. Georgiou, D. Veksler, J. T. Ryan, J. P. Campbell, P. R. Shrestha, and D. E. Ioannou, "Highly efficient rapid annealing of thin polar polymer film ferroelectric devices at sub-glass transition temperature," *Advanced Functional Materials*, vol. 28, no. 8, p. 1704165, 2018.
- [6] R. K. Kotnala, G. S. Arya, J. Yogiraj, and N. S. Negi, "Strain-induced structural, magnetic and ferroelectric properties of heterostructure BST–NZFO nanocomposite thin film at room temperature," *Bulletin of Materials Science*, vol. 40, no. 4, pp. 623–630, 2017.
- [7] F. Zhen, J. Deng, J. Wang, Z. Liu, P. Yang, and J. Xiao, "Ferroelectricity emerging in strained (111)-textured ZrO_2 thin films," *Applied Physics Letters*, vol. 108, no. 1, p. 012906, 2016.
- [8] F. Zhen, J. Chen, and J. Wang, "Ferroelectric hafnium dioxide-based materials for next-generation ferroelectric memories," *Journal of Advanced Dielectrics*, vol. 6, no. 2, pp. 1153–1156, 2016.
- [9] J. Shan, Y. Tang, X. Zhao, T. Wang, Z. Duan, and F. Wang, "Growth and electrical properties of epitaxial $0.7\text{Pb}(\text{Mg}_{1/3}\text{Nb}_{2/3})\text{O}_3\text{-}0.3\text{PbTiO}_3$ thin film by pulsed laser deposition," *Journal of Materials Science Materials in Electronics*, vol. 29, no. 8, pp. 6779–6784, 2018.
- [10] S. Sharma, P. Saravanan, O. P. Pandey, and P. Sharma, "Grain size distribution dependent magnetic and ferroelectric properties in sol-gel driven BiFeO_3 thin films," *Journal of Materials Science Materials in Electronics*, vol. 27, no. 6, pp. 5909–5915, 2016.
- [11] N. Lee, J. Lee, T. Ryu, Y. Kim, Y. Lansac, and Y. H. Jang, "Doping graphene with ferroelectric β -PVDF polymer film: density functional theory calculation and molecular dynamics simulation," *Science of Advanced Materials*, vol. 6, no. 11, pp. 2422–2427, 2014.
- [12] L. Xie, L. Li, C. A. Heikes, Y. Zhang, Z. Hong, and P. Gao, "Giant ferroelectric polarization in ultrathin ferroelectrics via boundary-condition engineering," *Advanced Materials*, vol. 29, no. 30, p. 1701475, 2017.
- [13] T. Iamsasri, J. Guerrier, G. Esteves et al., "A Bayesian approach to modeling diffraction profiles and application to ferroelectric materials," *Journal of Applied Crystallography*, vol. 50, no. 1, pp. 211–220, 2017.
- [14] C. Le Paven, R. Benzerger, A. Ferri, D. Fasquelle, V. Laur, and L. Le Gendre, "Ferroelectric and dielectric study of strontium tantalum based perovskite oxynitride films deposited by reactive rf magnetron sputtering," *Materials Research Bulletin*, vol. 96, no. 2, pp. 126–132, 2017.
- [15] A. P. Chen, W. Lin, J. Chen, and Y. P. Feng, "Thickness and ferroelectric polarization influence on film magnetic anisotropy across a multiferroic material interface," *ACS Applied Materials and Interfaces*, vol. 12, no. 39, pp. 44317–44324, 2020.
- [16] L. P. Zhang, Z. L. Lv, J. P. Cao, G. L. Zhao, and Y. Jiang, "Enhanced ferroelectric and photoelectric properties in lead-free $\text{Bi}_{1.07}\text{FeO}_3$ -modified $\text{K}_{0.5}\text{Na}_{0.5}\text{NbO}_3$ thin films," *Journal of Materials Science: Materials in Electronics*, vol. 32, no. 47, pp. 2051–2060, 2021.
- [17] P. P. Biswas, C. Thirimal, S. Pal, M. Miryala, M. Murakami, and P. Murugavel, "The composition and poling-dependent photovoltaic studies in ferroelectric $(\text{Bi}_{1-x}\text{Sr}_x)(\text{Fe}_{1-x}\text{Ti}_x)\text{O}_3$ thin films," *Journal of Materials Science: Materials in Electronics*, vol. 31, no. 2, pp. 1515–1523, 2020.
- [18] T. Carlier, M. H. Chambrier, A. D. Costa, F. Blanchard, and A. Ferri, "Ferroelectric state in an α - Nd_2WO_6 polymorph stabilized in a thin film," *Chemistry of Materials*, vol. 32, no. 17, pp. 7188–7200, 2020.
- [19] A. I. Stognij, N. N. Novitskii, S. A. Sharko et al., "On the visualization of the magnetoelectric coupling region for a thin ferromagnetic layer on a ferroelectric substrate," *Inorganic Materials*, vol. 55, no. 3, pp. 284–289, 2019.
- [20] W. Xiao, C. Liu, Y. Peng, S. Zheng, and Y. Zhou, "Thermally stable and radiation hard ferroelectric $\text{Hf}_{0.5}\text{Zr}_{0.5}\text{O}_2$ thin films

- on muscovite mica for flexible nonvolatile memory applications,” *ACS Applied Electronic Materials*, vol. 1, no. 6, pp. 919–927, 2019.
- [21] K. D. Kim, Y. J. Kim, M. H. Park, H. W. Park, Y. J. Kwon, and Y. B. Lee, “Transient negative capacitance effect in atomic-layer-deposited $\text{Al}_2\text{O}_3/\text{Hf}_{0.3}\text{Zr}_{0.7}\text{O}_2$ bilayer thin film,” *Advanced Functional Materials*, vol. 29, no. 17, p. 1808228, 2019.
- [22] G. Panchal, R. J. Choudhary, and D. M. Phase, “Magnetic properties of $\text{La}_{0.7}\text{Sr}_{0.3}\text{MnO}_3$ film on ferroelectric BaTiO_3 substrate,” *Journal of Magnetism & Magnetic Materials*, vol. 448, pp. 262–265, 2018.
- [23] J. Seo, J. Y. Son, and W. H. Kim, “Piezoelectric and ferroelectric characteristics of P(VDF-TrFE) thin films on Pt and ITO substrates,” *Materials Letters*, vol. 238, no. 1, pp. 237–240, 2018.
- [24] X. Guo, Y. Chen, G. Wang, W. Zhang, J. Lian, and X. Dong, “Investigation of novel ferroelectric/gyromagnetic ferrite $(\text{Pb,Sr})\text{TiO}_3/\text{Y}_3\text{Fe}_5\text{O}_{12}$ layered thin films with potential applications in magnetically and electrically tuning devices,” *Materials Letters*, vol. 195, no. 15, pp. 182–185, 2017.
- [25] H. Wang, F. Khatkhatay, J. Jian, J. Huang, M. Fan, and H. Wang, “Strain tuning of ferroelectric and optical properties of rhombohedral-like BiFeO_3 thin films on SrRuO_3 -buffered substrates,” *Materials Research Bulletin*, vol. 110, pp. 120–125, 2019.
- [26] Q. Luo, H. Ma, H. Su, K. H. Xue, and M. Liu, “Composition-dependent ferroelectric properties in sputtered HfXZr1-XO_2 thin films,” *IEEE Electron Device Letters*, vol. 40, no. 4, pp. 570–573, 2019.
- [27] A. S. Sidorkin, L. P. Nesterenko, B. M. Darinskii et al., “Switching processes of thin ferroelectric films,” *Materials Research Bulletin*, vol. 96, no. 3, pp. 206–210, 2017.